Supplement of The Cryosphere, 19, 4855–4873, 2025
https://doi.org/10.5194/tc-19-4855-2025-supplement

The Cryosphere Open Access EGU

Supplement of

Quantifying retrogressive thaw slump mass wasting and carbon mobilisation on the Qinghai-Tibet Plateau using multi-modal remote sensing

Kathrin Maier et al.

Correspondence to: Kathrin Maier (maierk@ethz.ch)

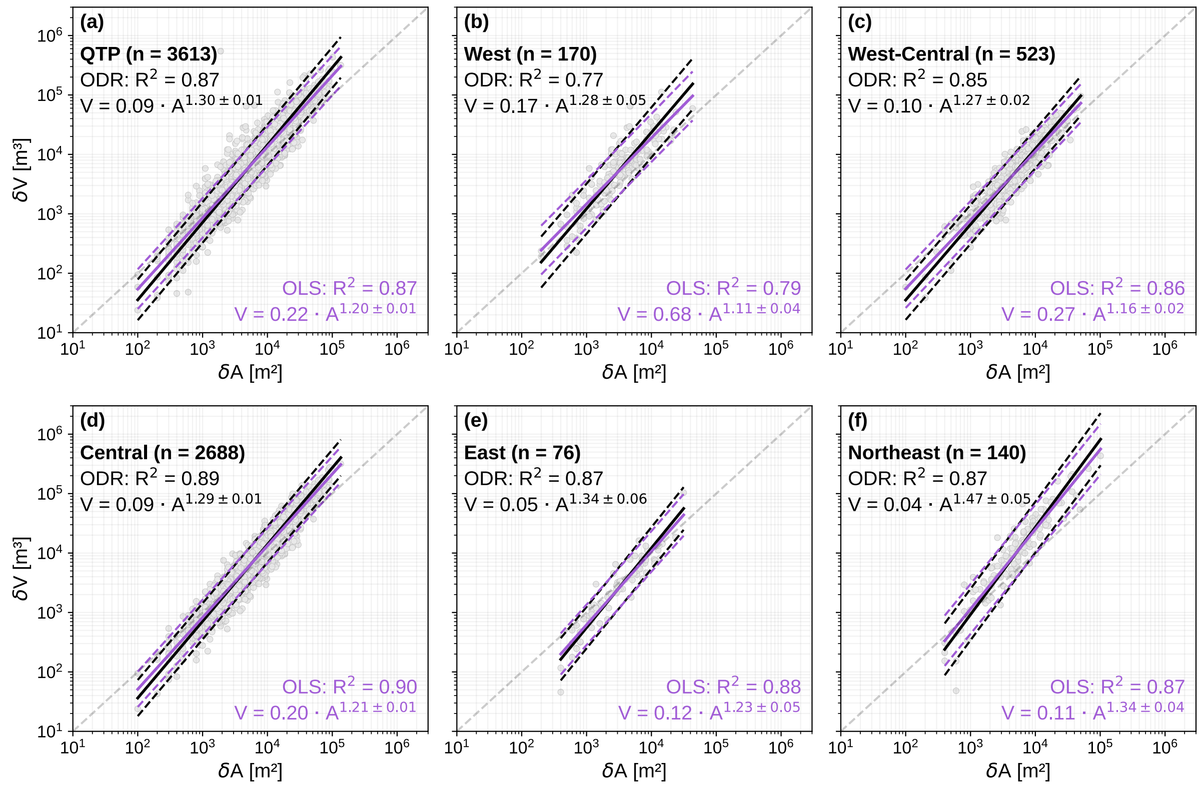

Figure S1: Allometric scaling between the actively eroding area of the delineations of the RTS inventory δA and the computed volume change based on the negative elevation change of the TanDEM-X DEM (T1 - T2) computed with OLS (in purple) and with ODR (in black). **(a)** For the entire QTP with n_{RTS} = 3613, we found scaling coefficients $\alpha_{ODR} = 1.30 \pm 0.01$ with $R^2 = 0.87$ and $\alpha_{OLS} = 1.20 \pm 0.01$ with $R^2 = 0.87$. **(b) – (f)** For the QTP subregions, we found values of α_{ODR} between 1.27 and 1.47 with R^2-values between 0.77 and 0.89 and of α_{OLS} between 1.11 and 1.34 with R^2-values between 0.79 and 0.90.

Table S1a: Detailed results of RTS activity between 2011 and 2020 on the QTP and in its subregions. We report the median quantities per RTS including entire RTS inventory area A_{Xia}, ablation area δA of the delineation, median and maximum (95th percentile) elevation change δh_{median} and δh_{max}, and volume change of thawed material δv, as well as the total estimates as the sum over all RTS per region including the volume change of erosion material δV (lower and upper bounds $\delta V^{-/+}$).

		Per RTS					Total		
	n	A_{Xia}	δA	δh_{median}	δh_{max}	δV	δV	δV^-	δV^+
Region		[10^3 m²]		[m]		[10^3 m³]		[10^6 m³]	
West	170	4.45	2.75	1.65	4.80	5.74	1.60	0.10	12.09
West-Central	523	6.80	4.20	1.01	2.04	4.73	4.14	0.31	39.55
Central	2688	8.70	5.80	1.22	2.32	6.89	39.28	5.56	178.52
East	76	4.55	2.90	0.84	1.85	2.48	0.40	0.05	3.50
Northeast	140	9.15	5.50	2.21	4.99	12.90	4.29	1.43	16.47
QTP	**3613**	**8.00**	**5.20**	**1.21**	**2.54**	**6.33**	**50.24**	**7.46**	**253.49**

Table S1b: Detailed results of RTS-induced GI loss and SOC mobilisation between 2011 and 2020 on the QTP and in its subregions. We report the total GI loss δGI and its lower and upper bounds $\delta GI^{-/+}$, the total amount of SOC that has been mobilised δSOC including lower and upper bounds $\delta SOC^{-/+}$, as well as the annual SOC rates $\delta SOC_{an.}$ (lower and upper bounds $\delta SOC_{an.}^{-/+}$) that represent δSOC normalised by the number of years of the temporal baseline of the DEM.

	δGI	δGI^-	δGI^+	δSOC	δSOC^-	δSOC^+	$\delta SOC_{an.}$	$\delta SOC_{an.}^-$	$\delta SOC_{an.}^+$
Region		[10^5 m^3]			[10^7 kg C]			[10^6 kg C a^{-1}]	
West	0.64	0.04	6.15	0.35	0.00	1.70	0.42	0.00	2.09
West-Central	1.96	0.12	32.28	1.76	0.00	7.35	2.27	0.00	9.43
Central	31.94	2.29	232.85	22.63	0.41	62.57	28.58	0.52	79.13
East	0.19	<0.01	4.37	0.54	<0.01	1.87	0.67	<0.01	2.31
Northeast	1.05	0.32	4.26	2.26	0.69	5.27	3.05	0.95	7.04
QTP	**35.81**	**2.80**	**281.99**	**27.83**	**1.11**	**79.80**	**35.34**	**1.47**	**101.28**

Table S2a: Number of detected RTS at the five validation sites (Fig. 1a) in (1) the RTS inventory of Xia et al. (2024) of 2019 and (2) manually identified in the elevation change maps based on TanDEM-X DEMs (2011-2019).

	Validation site	n_{RTS} for 2019 in RTS inventory of Xia et al. (2024)	n_{RTS} (2011-2019) in TanDEM-X elevation maps
A	Western Kunlun	121	44
B	Gaize	9	6
C	Southern Nima	4	4
D	Beiluhe River Basin	283	219
E	Qilian Mountain	28	17
Total		**445**	**290**

Table S2b: Validation of the planimetric area and material erosion volume estimated based on delineations of the RTS inventory from summer 2018, 2019, and 2020 and the elevation change between TanDEM-X DEMs (2011-2019). We report the estimated ablation area estimated from the inventory overlapping only negative elevation change δA for 2018, 2019, and 2020 as well as the volume change of the eroded material δV (including the propagated height error σ_v). The validation δA and δV values come from a manual delineation of the negative elevation change for 307 RTS at the five validation sites.

	δA [10^5 m^2]				$\delta V \pm \sigma_v$ [10^5 m^3]			
Test site	val.	2018	2019	2020	val.	2018	2019	2020
A Western Kunlun	2.20	4.75	5.00	5.37	9.19 ± 1.59	10.42 ± 3.97	11.01 ± 4.19	11.83 ± 4.43
B Gaize	0.23	0.22	0.25	0.27	0.44 ± 0.13	0.38 ± 0.15	0.43 ± 0.16	0.46 ± 0.16
C Southern Nima	2.14	2.18	2.30	2.39	3.70 ± 0.40	3.30 ± 0.40	3.46 ± 0.41	3.57 ± 0.42
D Beiluhe River Basin	36.04	33.74	41.80	49.20	78.58 ± 8.10	62.58 ± 8.46	76.09 ± 9.77	84.65 ± 10.52
E Qilian Mountain	1.68	2.84	3.31	3.54	7.48 ± 1.63	7.99 ± 2.58	8.83 ± 3.04	9.19 ± 3.08
All test sites	**42.28**	**43.72**	**52.65**	**60.77**	**99.39 ± 11.84**	**84.66 ± 15.55**	**99.81 ± 17.56**	**109.69 ± 18.61**

Table S3: Comparison between VHR DEMs based on a drone photogrammetric survey in summer 2020 at six RTS in the Beiluhe River Basin in the central QTP and the elevation change computed from the boundaries of the RTS inventory and the TanDEM-X DEM (2011-2019). The median headwall height is a direct measurement of the differences from elevations in undisturbed terrain and elevations from the slump floor close to the headwall in the VHR DEMs and indirectly computed for the TanDEM-X elevation change by dividing the volume change of the eroded material δV by the erosion affected area δA. The maximum elevation change within the RTS ablation area gives an indication of the potential headwall height and is used for the comparison to the VHR DEMs. For all values, we report the standard deviation / error estimate σ.

RTS	Location	Initiation	RTS area Total [m²]	RTS area Active [%]	VHR $\bar{h}$ [m]	TanDEM-X δh_{max} [m]
1	34.647° N, 92.936° E	2017	7265	77	2.76 ± 1.19	3.04 ± 1.91
2	34.731° N, 92.871° E	2017	9141	78	3.08 ± 1.06	3.78 ± 2.57
3	34.710° N, 92.887° E	2017	2536	81	1.10 ± 0.83	2.93 ± 1.85
4	34.708° N, 92.883° E	2017	9637	53	3.55 ± 0.75	3.83 ± 2.78
5	34.647° N, 92.928° E	2019	3891	69	1.99 ± 1.99	3.32 ± 2.46
6	34.646° N, 92.926° E	2019	1087	100	1.89 ± 0.98	1.83 ± 1.56

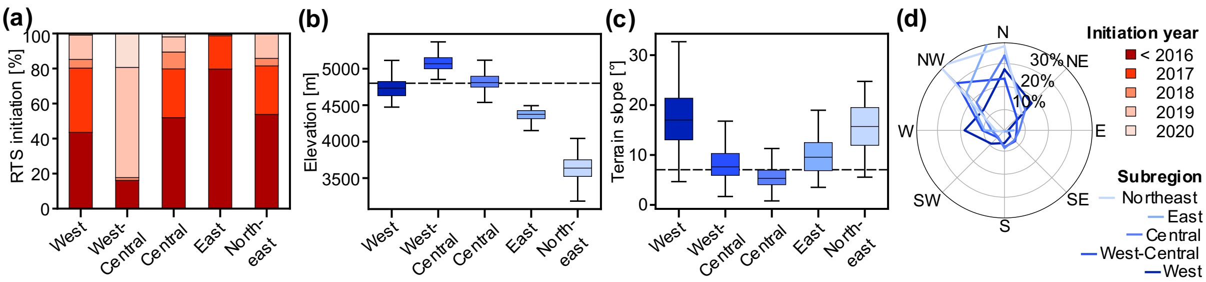

Figure S2: Temporal and terrain characteristics of RTS present in the optical inventory of Xia et al. (2024) in the subregions of QTP. **(a)** Percentage of RTS per initiation year. **(b)** Distribution of elevation of the RTS location. **(c)** Distribution of the slope of the average terrain at the RTS location. **(d)** Main terrain aspect of RTS.

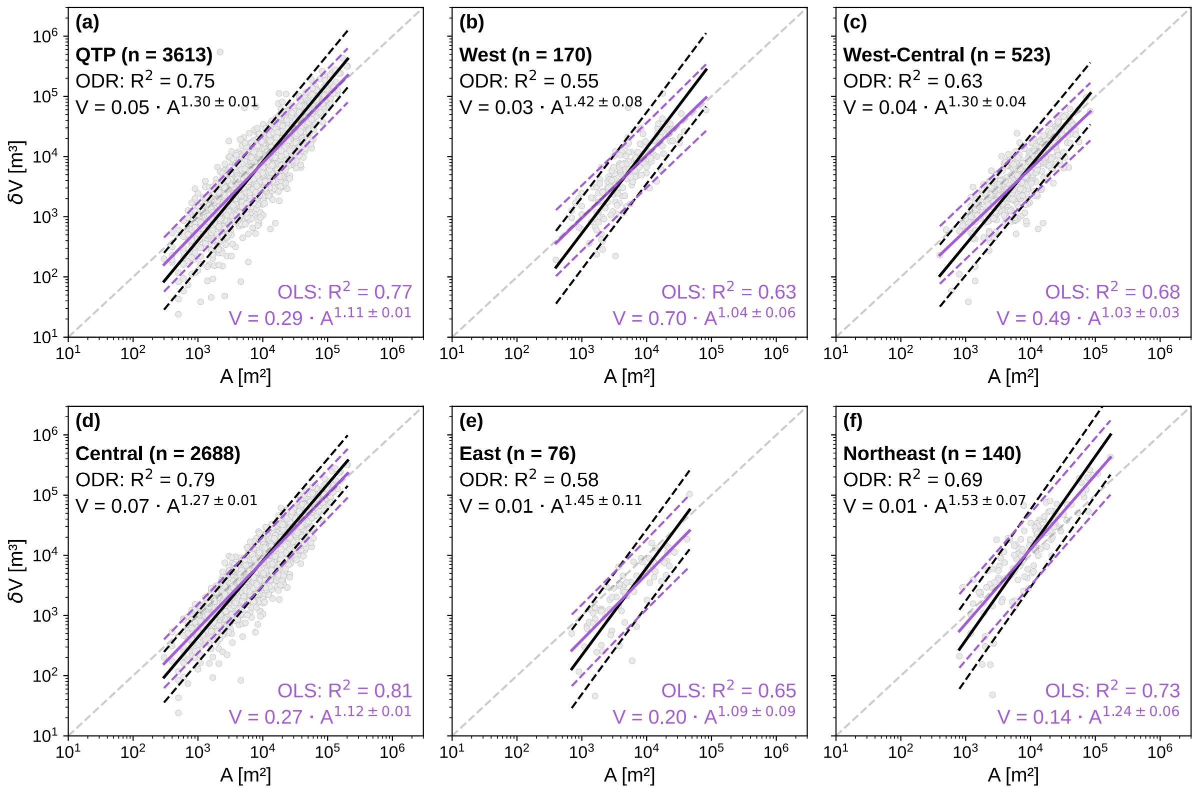

Figure S3: Allometric scaling between the entire area of the delineated scar zone A_{Xia} of the RTS inventory and the computed volume change based on the elevation change of the TanDEM-X DEMs within the ablation area computed with OLS (in purple) and with ODR (in black). **(a)** For the entire QTP with n_{RTS} = 3613, we found a scaling coefficient α_{ODR} = 1.30 ± 0.01 with R^2 = 0.75 and α_{OLS} = 1.11 ± 0.01 with R^2 = 0.77. **(b) – (f)** In the QTP subregions, we found scaling coefficients of α_{OLS} between 1.03 to 1.12 and of α_{ODR} between 1.27 and 1.45 in the QTP's central, western and eastern regions and higher scaling coefficients of α_{ODR} = 1.53 (R^2 = 0.69) and α_{OLS} = 1.24 (R^2 = 0.73) on the mountainous northeastern plateau.